HPU2 Journal of Sciences:
Natural Sciences and Technology

Journal homepage: https://sj.hpu2.edu.vn

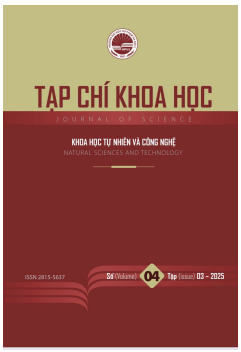

Article type: Research article

The synthesis of TiO_2 nanosheets and their outperformance in the photocatalytic degradation of methylene blue

Duc-Nam Cao[a], Ba-Trang Doan[a], Van-Tuan Mai[b,c], Dinh-Lam Nguyen[c], Duy-Khanh Nguyen[d], Minh-Quy Bui[d], Xuan-Dung Mai[a*]

[a]*Hanoi Pedagogical University 2, Phu Tho, Vietnam*
[b]*Electric Power University, Hanoi, Vietnam*
[c]*VNU-University of Engineering and Technology, Hanoi, Vietnam*
[d]*Thai Nguyen University of Sciences, Thai Nguyen, Vietnam*

Abstract

TiO_2 nanocrystals have been deployed as photocatalysts for the degradation of organic pollutants in wastewater due to their high chemical resistance and environmental friendliness. Because the reaction takes place on the catalyst surface, the crystal phase and the morphology of TiO_2 nanocrystals are important factors governing the catalytic activity. Herein, we prepared TiO_2 nanosheets by hydrothermal treatment of titanium (IV) butoxide in the presence of hydrofluoric acid. The crystallinity and the morphology of TiO_2 nanosheets were characterized by X-ray diffraction and scanning electron microscope (SEM), respectively. The photocatalytic activity of TiO_2 nanosheets was compared with that of commercially available TiO_2 nanoparticles (Degussa P25) using the degradation reaction of methylene blue (MB) in water under ultraviolet light at 365 nm. The X-ray diffraction and SEM characterizations indicated that anatase TiO_2 nanosheets with enriched {001} facets were successfully obtained. The MB degradation assay revealed that the decolorization of MB on TiO_2 nanosheets was 1.85 times faster than that on the TiO_2 nanoparticles counterpart. The synthesis and excellent photocatalytic activity of TiO_2 nanosheets demonstrated in this paper may promote the development of catalysts for removing organic pollutants in wastewater.

Keywords: TiO_2, nanosheets, photocatalyst, methylene blue, facet engineering

* Corresponding author, E-mail: maixuandung@hpu2.edu.vn

https://doi.org/10.56764/hpu2.jos.2025.4.3.26-33

Received date: 11-8-2025 ; Revised date: 18-9-2025 ; Accepted date: 22-11-2025

1. Introduction

Organic compounds, mainly dyes and pesticides, are one of the main pollutants in water. Nowadays, about one million metric tons of dyes are produced per year worldwide for the usage in various industries, particularly in paper, textile, rubber, leather, plastic, food, and drug factories [1]. Wastewater containing dyes discharged from industries may cause serious health problems because dyes are potentially toxic, carcinogenic, and mutagenic. Additionally, dyes are usually stable to light and heat and have a high resistance to oxidation and biodegradation [2]. Therefore, it is necessary for the development of advanced materials and technologies for the removal of organic pollutants, especially organic dyes, in industrial wastewater. Currently, there are three strategies for dye removal from wastewater including physical, chemical, and biological methods [1], [2]. Physical methods include adsorption [3], ion exchange, electro-coagulation, irradiation, and membrane filtration, all of which have common limitations in long contact time and frequent regeneration of materials [4], [5]. In biological methods, suitable fungi, plant, bacteria, or microorganisms are used to digest dyes in aerobic or anaerobic treatments. Those biological methods have advantages of low energy consumption and being environmentally friendly, but they need steady conditions and require a long treatment time. Chemical methods including precipitation, Fenton, ozonation, and photocatalysis can degrade different types of dyes in a shorter time but they require suitable materials. Among chemical methods, photocatalysis can operate at middle conditions while give high degradation efficiency even at low dye concentrations [6]. Those advantages of photocatalytic methods are based on the formation of extremely reactive superoxide and hydroxyl radicals followed by photoexcitation of photocatalyst [6].

TiO_2 is a chemically and biologically inert [7], non-toxic, inexpensive, and viable semiconductor that has been emerged as an advantageous photocatalyst for dye removal. Naturally, TiO_2 exits in anatase, rutile, or brookite phases [8]–[10] of which anatase has been debated to have the highest photocatalytic activity. Anatase TiO_2 of different morphologies has been widely used as photocatalyst for dyes degradation [11]–[13]. In the photocatalysis, light absorption generates excited electron (e^-) and hole (h^+), which stabilize respectively at the conduction band edge and the valence band edge of TiO_2 [14]. e^- reacts with adsorbed oxygen to form superoxide radical while h^+ reacts with water forming hydroxyl radical [15]. The resulting radicals initiate the oxidation degradation of the toxic dyes. Therefore, the photocatalytic activity of TiO_2 depends on its surface area, surface finishing facets, the lifetime of excited e^- and h^+, and the energy levels of the band edges.

One of the strategies to increase the photocatalytic activity of TiO_2 is to enhance oxygen adsorption on its surface by which the formation of superoxide is promoted. Theoretical calculations suggest {001} facet to have the highest adsorption affinity to oxygen [16]. Recently, although anatase TiO_2 materials with enhanced {001} facet have been increasingly studied for dyes removal [11], [15], [17]–[19] a direct comparison in the photocatalytic activity with the well-known Degussa P25 has not reported yet. Herein, we present a simple method for the synthesis of anatase TiO_2 nanosheets with enhanced {001} finishing facet. Compared to commercial Degussa P25 the nanosheets have a better photocatalytic activity in methylene blue degradation.

2. Materials and Methods

2.1. Chemicals and instruments.

Degussa P25 which contains nanoparticles (TiO_2 NPs) having a diameter smaller than 100 nm was purchased from Aladdin Chemicals and used as reference photocatalyst. Titanium (IV) butoxide

($Ti(OC_4H_9)_4$, 98%) and hydrofluoric acid (HF, 48%) were received from Aladdin Chemicals and used directly without any purifications. Instruments include a 50 ml PPL (para-polyphenylene) lined in autoclave, a temperature-controllable oven, and a centrifuge. A home-made photoreactor was set up using 3W UV LEDs emitting at 365 nm, a power supplier, a three-neck flask equipped with a condenser, quartz tube for inserting the UV LEDs, a syringe for sampling, and a magnetic stirrer.

2.2. The synthesis of TiO_2 nanosheets

0.8 ml of HF solution was added dropwise into a 20 ml plastic vial containing 5 ml of $Ti(BO)_4$ while being stirred. The mixture was transferred into an autoclave and placed in an electric oven at 200°C for 24 hours. After the hydrothermal treatment, TiO_2 powder was washed thoroughly with water before being aged in NaOH solution (0.5 M) for 30 minutes. After aging, the powder was washed again with water, acetone, and dried at 120°C for 30 minutes to obtain TiO_2 nanosheets.

2.3. Characterizations

The crystallinity of TiO_2 nanosheets was studied by X-ray diffraction method which was conducted on D8 Advance Eco (Bruker – Germany). The morphology of TiO_2 nanosheets was investigated by scanning electron microscope (SEM) technique which was conducted on a JSM-IT200 (JEOL-Japan). UV-Vis absorption spectra of methylene blue solutions were recorded on a 6715 UV/Vis spectrophotometer (Jenway, USA).

2.4. Photocatalytic assay

0.1 g of TiO_2 nanosheets or the reference catalyst (Degussa P25) was added to the photoreactor containing 100 ml of MB solution (10 mg/L). The mixture was stirred in the dark condition for 30 minutes for adsorption equilibrium. After that the UV LEDs were turned on via a power supplier that worked at a voltage of 3.5 V and a current of 0.2 A (total output power of 0.7 W). After different reaction times, 3 ml of reaction mixture was taken and filtered through a 0.21 μm syringe filter to get MB solutions. The concentration of MB was evaluated using a standard equation and its absorbance at 663 nm. The standard equation was experimentally established using a series absorbance at 663 nm of standard MB solutions. The degradation rate of MB was fitted to 1-order reaction (equation 1), in which C_0 and C_t are the concentrations of MB at the initial state and at reaction time of t, respectively; k is the rate constant.

$$\ln\frac{C_0}{C_t} = kt \tag{1}$$

3. Results and Discussion

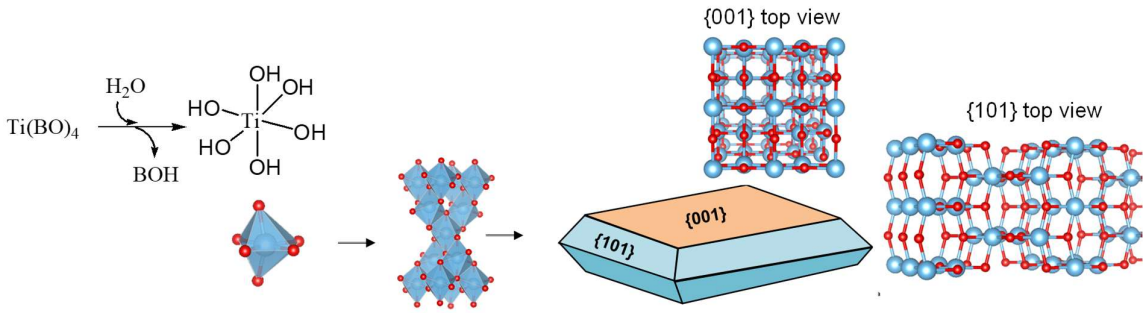

Figure 1. The formation of anatase TiO_2 nanosheets.

Upon dissolving $Ti(BO)_4$ into HF solution, $Ti(BO)_4$ undergoes hydrolysis processes, equation (2), where *x* increases from 1 to 4 depending on water content and reaction time.

$$Ti(BO)_4 + xH_2O \rightarrow Ti(OH)_x(BO)_{4-x} + xBOH \quad (2)$$

In the presence of fluoride ions (F^-), they could replace the original hydroxyl (OH^-) or butoxyl (BO) ligand surrounding Ti, equation (3).

$$Ti(OH)_x(BO)_{4-x} + yF^- \rightarrow Ti(OH)_x F_y(BO)_{4-x-y} \quad (3)$$

Additionally, water also bonds to Ti forming octahedrons, equation (4).

$$Ti(OH)_x F_y(BO)_{4-x-y} + (6-x-y-z)H_2O \rightarrow Ti(OH)_x F_y(BO)_z(H_2O)_{6-x-y-z} \quad (4)$$

For simplicity, we used $\left[Ti(OH)_6\right]^{2-}$ to represent the Ti-octahedron in Figure 1. It is worthy mentioning that $\left[Ti(OH)_6\right]^{2-}$ is an ideal formula to represent the product of the hydrolysis process. In fact, $Ti(OH)_{x\leq 6}$ tends to condensate together forming oxide network [20], equation (5).

$$TiOH + TiOH \rightarrow Ti-O-Ti + H_2O \quad (5)$$

Shortly, the assembly of Ti-octahedron in hydrothermal conditions leads to the formation of TiO_2. It has been demonstrated that the surface energy of TiO_2 for different facets is in order {001} (0.9 J/m^2), {100} (0.53 J/m^2), and {101} (0.44 J/m^2) [21]. Thermodynamically, the growth of TiO_2 is preferred toward the formation of anatase TiO_2 having dominant finishing {101} facet. In the presence of fluoride ions, as in the current case, they would replace the surface hydroxyl to reduce the surface energy [22]. Importantly, fluorinated {001} facet becomes more stable than {101} facet. As a result, the growth of TiO_2 is induced toward the formation of anatase TiO_2 with enriched {001} facet as illustrated in Figure 1. Finally, the surface fluoride ions are replaced by hydroxyl via the NaOH treatment (see experiment section).

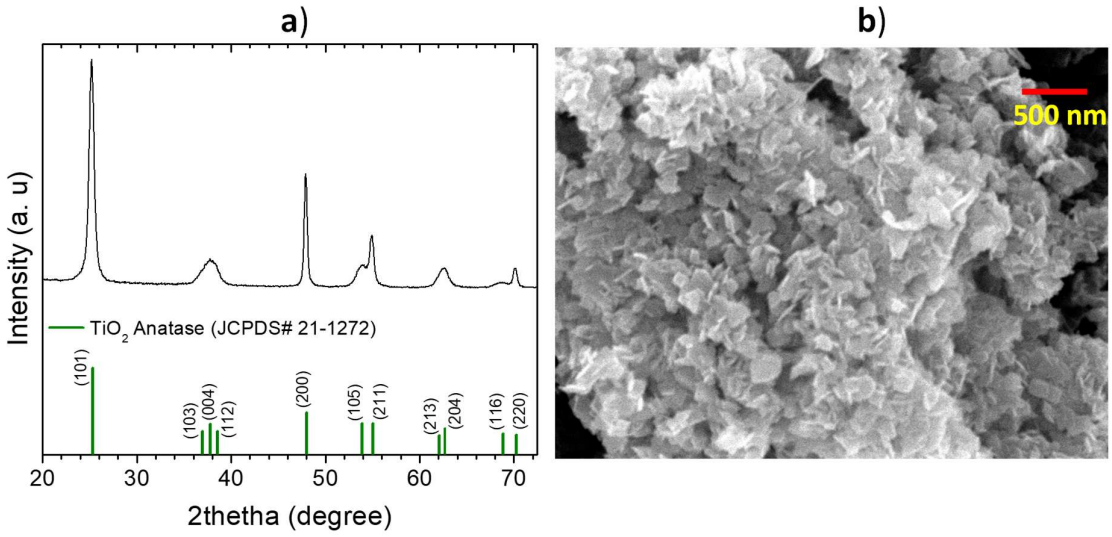

Figure 2. a) X-ray diffraction pattern and **b**) SEM image of anatase TiO_2 nanosheets.

The formation of anatase TiO_2 nanosheets was confirmed by X-ray diffraction and SEM characterizations, Figure 2. The diffraction pattern of TiO_2 product shown in Figure 2**a** exhibits diffraction

peaks at 2thetha of 25.3, 37.8, 48.0, and 53.9° which are attributed accordingly to the diffraction from (101), (004), (200), and (105) planes of anatase phase (JCPDS# 21-1272) [11], [15], [23], [24]. The identical in diffraction peaks between TiO_2 product and the standard anatase indicates that the product was anatase TiO_2. Furthermore, SEM image, shown in Fig 2**b**, reveals that TiO_2 product consists of individual sheets with an average length (L) of about 120 nm and an average thickness (T) of 20 nm. In summary, anatase TiO_2 nanosheets were successfully synthesized.

The ratio of {001} facet (P_{001}) in final anatase TiO_2 nanosheets was estimated to be about 71.5% by using equation (6)-(8), where S_{001} and S_{101} are the total surface of {001} and {101} facets, respectively; θ = 68.3° is the angle between the {001} and {101} facets in anatase [11], [12].

$$S_{001} = 2\left(L - \frac{T}{\tan\theta}\right)^2 \tag{6}$$

$$S_{101} = \frac{2T}{\sin\theta}\left(2L - \frac{T}{\tan\theta}\right) \tag{7}$$

$$P_{001} = \frac{S_{001}}{S_{001} + S_{101}} \tag{8}$$

The anatase TiO_2 nanosheets with enriched {001} facet whose surface energy and oxygen adsorption affinity is high are expected to have high photocatalytic activity. The photocatalytic activity of TiO_2 nanosheets was compared with that of commercially available Degussa P25 (TiO_2 NPs) using a UV-induced MB degradation reaction. The change in MB concentration over time was measured by an absorption method. First, we established a standard equation between MB concentration (C_{MB}) and the absorbance at 663 nm (Abs) where MB has the highest absorption coefficient as shown in Figure 3**a**. The correlation between C_{MB} and Abs in 1-10 mg/L range is shown in Figure 3**b**. The experimental data was well fitted by equation (9) with a coefficient of determination R^2 of 99.86%.

$$C_{MB} = 4.6898 Abs;\ R^2 = 99.86\% \tag{9}$$

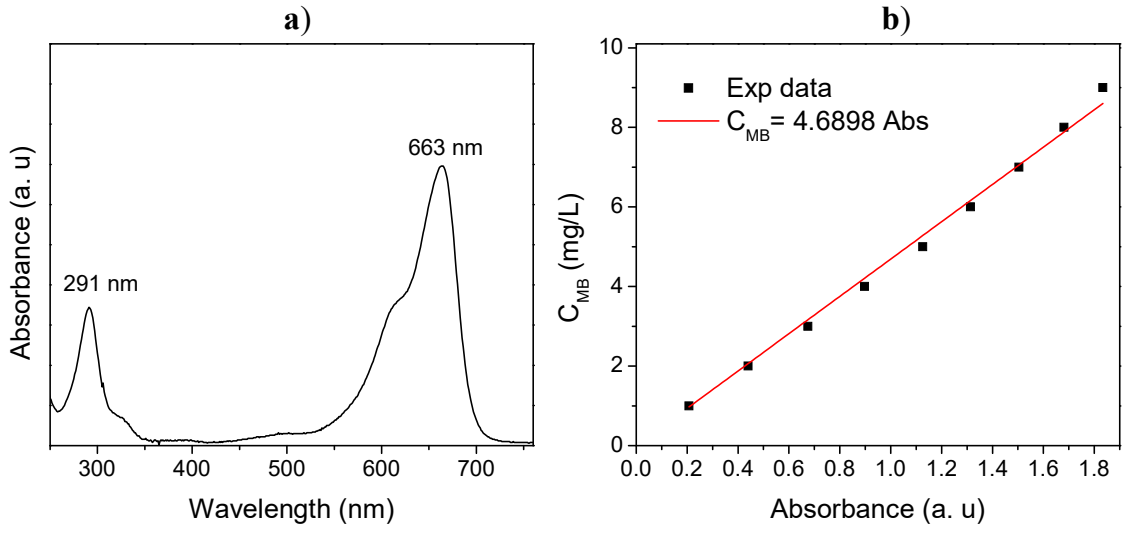

Figure 3. **a**) The UV-Vis absorption spectrum of MB and **b**) The correlation between MB concentration and the absorbance at 663 nm.

Next, the concentrations of MB at various of reaction times were extrapolated using the absorbance of MB sample solutions and equation (9), the results are shown in Figure 4. During dark state, where the adsorption of MB on solid catalysts occurred, more MB was absorbed by TiO_2 NPs than TiO_2 nanosheets. Concisely, 47.5% of MB was removed by adsorption on TiO_2 NPs while that on TiO_2 nanosheets was only 6.5%, Figure 4**b**. Under UV irradiation, the concentration of MB decreased gradually in both cases and the degradation rate was faster on TiO_2 nanosheets, Figure 4**a**. Accordingly, the removal of MB was increased with time and TiO_2 nanosheets became more effective after 12 hours, Figure 4**b**.

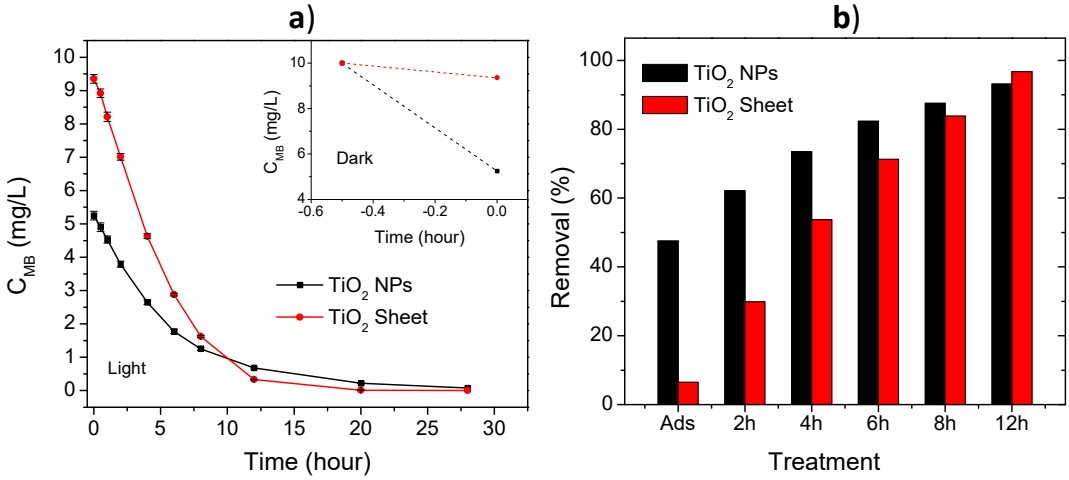

Figure 4. **a**) The variation of MB concentration upon photocatalysis on anatase TiO_2 nanosheets (TiO_2 Sheet) or commercial Degussa P25 (TiO_2 NPs). Inset in **a**) the change in MB concentration due to adsorption. **b**) The removal of MB from water after different treatment time.

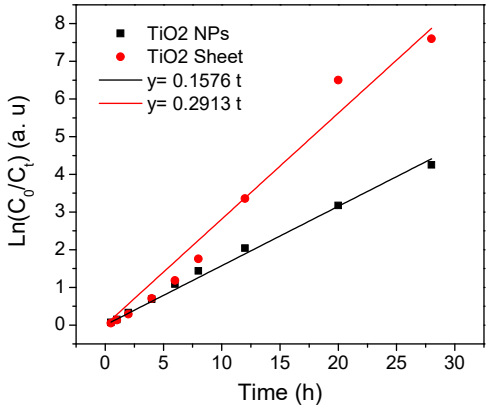

Figure 5. Fitting the degradation of MB according to the first-order reaction.

To study the kinetic of the degradation reaction of MB on different photocatalyst, we fitted the experiment data to the first-order reaction, equation (1). The results are shown in Figure 5. Apparently, the degradation of MB on photocatalysts was well-fitted to the first-order reaction with very good coefficients of determination, equation (10) and (11). The photo-induced, first-order degradation of MB has been reported widely for different catalysts [12], [18], [23], [25]–[29]. The rate constant of TiO_2 nanosheets (0.2913 $hour^{-1}$) was 1.85 times greater than that of TiO_2 NPs (0.1575 $hour^{-1}$). Notably, the rate constants in our case cannot be compared directly with other reports [12], [23] because of the differences

in experimental details, such as light wavelength, light intensity, reaction reactor, and the distance between the light source and MB solution. However, with identical MB degradation assay, we surely conclude that the anatase TiO_2 nanosheets has a higher photocatalytic activity than reference TiO_2 NPs.

$$\ln\left(\frac{C_0}{C}\right) = 0.1576t; \quad R^2 = 99.68\% \tag{10}$$

$$\ln\left(\frac{C_0}{C}\right) = 0.2913t; \quad R^2 = 98.42\% \tag{11}$$

4. Conclusions

Anatase TiO_2 nanosheets were successfully synthesized by hydrothermal treatment of $Ti(BO)_4$ in the presence of HF. The product was 120 nm-long and 20 nm-thick nanosheets that have 71.5% of the surface covered by high-energy {001} facet. The potential application of the TiO_2 nanosheets as a photocatalyst for dyes removal in wastewater was evaluated by comparison with well-known Degussa P25 via MB degradation reaction. Despite low MB adsorption capacity, the TiO_2 nanosheets exhibit much better photocatalytic activity than P25. The results demonstrated in this study suggest the importance of surface engineering in controlling the activity of photocatalysts and may motivate the development of effective photocatalysts for waste water treatment.

Acknowledgments

This research is funded by Hanoi Pedagogical University 2 Foundation for Sciences and Technology Development under Grant Number: SV.2025.HPU2.04

References

[1] M. F. Hanafi and N. Sapawe, "A review on the current techniques and technologies of organic pollutants removal from water/wastewater," *Mater. Today Proc.*, vol. 31, no. 2020, pp. A158–A165, Feb. 2021, doi: 10.1016/j.matpr.2021.01.265.

[2] A. A. Najim, A. Y. Radeef, and Z. H. Jabbar, "Recent trends in physio-chemo technologies and their role in dyes removal: Effectiveness, benefits, and limitations," *Chem. Eng. Res. Des.*, vol. 219, pp. 198–221, Jun., 2025, doi: 10.1016/j.cherd.2025.06.005.

[3] N. T. K. Trinh et al., "One-step synthesis of activated carbon from surgacane bagasse," *TNU J. Sci. Technol.*, vol. 226, no. 11, pp. 47–52, Jul. 2021, doi: 10.34238/tnu-jst.4479.

[4] N. T. Huyen, M. X. Dung, N. T. Duyen, and D. T. Tien, "Enhance the Cu(II) adsorption by cross-linking PEI on the surface of SiO_2," *TNU J. Sci. Technol.*, vol. 229, no. 10, pp. 68–75, May, 2024, doi: 10.34238/tnu-jst.9855.

[5] P. T. T. Thanh, L. Q. Mai, and M. X. Dung, "Conflicting effects of PEI grafting on the adsorption properties of activated carbon," *TNU J. Sci. Technol.*, vol. 229, no. 10, pp. 18–25, May 2024, doi: 10.34238/tnu-jst.9758.

[6] M. Ahtasham Iqbal et al., "Advanced photocatalysis as a viable and sustainable wastewater treatment process: A comprehensive review," *Environ. Res.*, vol. 253, May 2024, Art. no. 118947, doi: 10.1016/j.envres.2024.118947.

[7] V. C. Manh et al., "Study on coating of TiO_2 nanotubes on microporous Ti surfaces for biomedical applications," *Key Eng. Mater.*, vol. 1002, pp. 45–53, Dec. 2024, doi: 10.4028/p-xqj5HI.

[8] T. Tung Nguyen, X. D. Mai, and N. H. Duong, "Simultaneous synthesis of anatase colloidal and multiple-branched rutile TiO_2 nanostructures," *Bull. Korean Chem. Soc.*, vol. 38, no. 3, pp. 401–405, Jan. 2017, doi: 10.1002/bkcs.11101.

[9] D. R. Eddy et al., "Heterophase polymorph of TiO_2 (Anatase, Rutile, Brookite, TiO_2 (B)) for efficient photocatalyst: Fabrication and activity," *Nanomaterials*, vol. 13, no. 4, Feb. 2023, Art. no. 704, doi: 10.3390/nano13040704.

[10] H. D. Ngoc, D. M. Xuan, and T. M. Van, "Effect of pH on the formation of amorphous TiO_2 complexes and TiO_2 anatase during the pyrolysis of an aqueous $TiCl_4$ solution," *Catalysts*, vol. 10, no. 10, Oct. 2020, Art. no. 1187, doi: 10.3390/catal10101187.

[11] Y. Kowaka et al., "Development of TiO_2 nanosheets with high dye degradation performance by regulating crystal growth," *Materials*, vol. 16, no. 3, Jan. 2023, Art. no. 1229, doi: 10.3390/ma16031229.

[12] B. Li et al., "Enhanced visible-driven photocatalysis in black TiO_2 nanosheets with co-exposed {001} and {101} planes," *Surfaces and Interfaces*, vol. 59, Jan. 2025, Art. no. 105930, doi: 10.1016/j.surfin.2025.105930.

[13] S. P. Sabino et al., "Investigation of the photocatalytic activity of various TiO_2 nanoparticles in the contaminant remediation," J. *Environ. Chem. Eng*., vol. 8, Jan. 2025, Art. no. 100856, doi: 10.1016/j.nxmate.2025.100856.

[14] N. H. Duong, V. T. Mai, and X. D. Mai, "Charge photogeneration and transfer in polyaniline/titanium dioxide heterostructure," *Catalysts*, vol. 14, no. 9, Sep. 2024, Art. no. 585, doi: 10.3390/catal14090585.

[15] X. Zhou et al., "The effect of surface heterojunction between (001) and (101) facets on photocatalytic performance of anatase TiO_2," *Mater. Lett*., vol. 205, pp. 173–177, Jun. 2017, doi: 10.1016/j.matlet.2017.06.095.

[16] Y. Gao et al., "Unravelling the origin of facet-dependent photocatalytic H_2O_2 production over anatase TiO_2," *Mater. Today Energy*, vol. 40, Dec. 2023, Art. no. 101483, doi: 10.1016/j.mtener.2023.101483.

[17] S. Odabasi Lee, S. K. Lakhera, and K. Yong, "Strategies to enhance interfacial spatial charge separation for high-efficiency photocatalytic overall water-splitting: A review," *Adv. Energy Sustain. Res*., vol. 4, no. 12, Sep. 2023, Art. no. 2300130, doi: 10.1002/aesr.202300130.

[18] R. Liu et al., "Fabrication of {001}-facet enriched anatase TiO_2/$TiOF_2$ heterostructures with controllable morphology for enhanced photocatalytic activity," *Mater. Today Commun*., vol. 26, Jan. 2021, Art. no. 102060, doi: 10.1016/j.mtcomm.2021.102060.

[19] K. Chen et al., "Synthesis and improved photocatalytic activity of ultrathin TiO_2 nanosheets with nearly 100% exposed (001) facets," *Ceram. Int*., vol. 40, no. 10, pp. 16817–16823, Jul. 2014, doi: 10.1016/j.ceramint.2014.07.050.

[20] F. Wu, L. Fan, Y. Chen, S. Chen, J. Shen, and P. Liu, "Crystallization of 2D TiO_2 nanosheets via oriented attachment of 1d coordination polymer," *Nano Lett*., vol. 25, no. 1, pp. 56–62, Oct. 2024, doi: 10.1021/acs.nanolett.4c04084.

[21] X. Han, Q. Kuang, M. Jin, Z. Xie, and L. Zheng, "Synthesis of titania nanosheets with a high percentage of exposed (001) facets and related photocatalytic properties," *J. Am. Chem. Soc*., vol. 131, no. 9, pp. 3152–3153, Mar. 2009, doi: 10.1021/ja8092373.

[22] H. G. Yang et al., "Anatase TiO_2 single crystals with a large percentage of reactive facets," *Nature*, vol. 453, no. 7195, pp. 638–641, May 2008, doi: 10.1038/nature06964.

[23] S. P. Sabino, E. B. Santos, B. I. M. Santos, and M. Goncalves, "Investigation of the photocatalytic activity of various TiO_2 nanoparticles in the contaminant remediation," *Next Mater*., vol. 8, Jun. 2025, Art. no. 100856, doi: 10.1016/j.nxmate.2025.100856.

[24] K. Hayashi et al., "Enhanced antibacterial property of facet-engineered TiO_2 nanosheet in presence and absence of ultraviolet irradiation," *Materials*., vol. 13, no. 1, Dec. 2019, Art. no. 78, doi: 10.3390/ma13010078.

[25] G. B. Yitagesu, D. T. Leku, A. M. Seyume, and G. A. Workneh, "Biosynthesis of TiO_2/CuO and its application for the photocatalytic removal of the methylene blue dye," *ACS Omega*, vol. 9, no. 40, pp. 41301–41313, Sep. 2024, doi: 10.1021/acsomega.4c03472.

[26] Z. Liu, X. Liu, Q. Lu, Q. Wang, and Z. Ma, "$TiOF_2$/TiO_2 composite nanosheets: Effect of hydrothermal synthesis temperature on physicochemical properties and photocatalytic activity," *J. Taiwan Inst. Chem. Eng*., vol. 96, pp. 214–222, Nov. 2018, doi: 10.1016/j.jtice.2018.11.013.

[27] G. Zerjav, K. Zizek, J. Zavasnik, and A. Pintar, "Brookite vs. rutile vs. anatase: What's behind their various photocatalytic activities?," *J. Environ. Chem. Eng*., vol. 10, no. 3, Apr. 2022, Art. no. 107722, doi: 10.1016/j.jece.2022.107722.

[28] F. Bertolotti et al., "Structure, morphology, and faceting of TiO_2 photocatalysts by the Debye scattering equation method. The P25 and P90 cases of study," *Nanomaterials*, vol. 10, no. 4, Apr. 2020, Art. no. 743, doi: 10.3390/nano10040743.

[29] A. Trenczek-Zajac et al., "Scavenger-supported photocatalytic evidence of an extended type I electronic structure of the TiO_2@Fe_2O_3 interface," *ACS Appl. Mater. Interfaces*, vol. 14, no. 33, pp. 38255–38269, Aug. 2022, doi: 10.1021/acsami.2c06404.